Reinterpreting the Bruun Rule in the Context of Equilibrium Shoreline Models

Maurizio d'Anna, Déborah Idier, Bruno Castelle, Sean Vitousek, Goneri Le Cozannet

Journal of *Marine Science and Engineering*

MDPI

Article

Reinterpreting the Bruun Rule in the Context of Equilibrium Shoreline Models

Maurizio D'Anna [1,2,*], Deborah Idier [2], Bruno Castelle [1], Sean Vitousek [3] and Goneri Le Cozannet [2]

1 Le Centre National de la Recherche Scientifique (CNRS), Université de Bordeaux, UMR EPOC, Allée Geoffrey Saint-Hilaire, 33615 Pessac, France; bruno.castelle@u-bordeaux.fr
2 BRGM, French Geological Survey, 3 Av. Guillemin, 45060 Orléans, France; d.idier@brgm.fr (D.I.); g.lecozannet@brgm.fr (G.L.C.)
3 US Geological Survey, 2885 Mission Street, Santa Cruz, CA 95060, USA; svitousek@usgs.gov
* Correspondence: maurizio.danna@u-bordeaux.fr

Abstract: Long-term (>decades) coastal recession due to sea-level rise (SLR) has been estimated using the Bruun Rule for nearly six decades. Equilibrium-based shoreline models have been shown to skillfully predict short-term wave-driven shoreline change on time scales of hours to decades. Both the Bruun Rule and equilibrium shoreline models rely on the equilibrium beach theory, which states that the beach profile shape equilibrates with its local wave and sea-level conditions. Integrating these two models into a unified framework can improve our understanding and predictive skill of future shoreline behavior. However, given that both models account for wave action, but over different time scales, a critical re-examination of the SLR-driven recession process is needed. We present a novel physical interpretation of the beach response to sea-level rise, identifying two main contributing processes: passive flooding and increased wave-driven erosion efficiency. Using this new concept, we analyze the integration of SLR-driven recession into equilibrium shoreline models and, with an idealized test case, show that the physical mechanisms underpinning the Bruun Rule are explicitly described within our integrated model. Finally, we discuss the possible advantages of integrating SLR-driven recession models within equilibrium-based models with dynamic feedbacks and the broader implications for coupling with hybrid shoreline models.

Keywords: sea-level rise; Bruun Rule; equilibrium shoreline models; passive flooding; wave energy efficiency

Citation: D'Anna, M.; Idier, D.; Castelle, B.; Vitousek, S.; Le Cozannet, G. Reinterpreting the Bruun Rule in the Context of Equilibrium Shoreline Models. *J. Mar. Sci. Eng.* **2021**, *9*, 974. https://doi.org/10.3390/jmse9090974

Academic Editor: Alessandro Antonini

Received: 4 August 2021
Accepted: 31 August 2021
Published: 7 September 2021

1. Introduction

Sandy beaches are dynamic environments, responding to a variety of complex processes interacting on different temporal and spatial scales [1]. As sea-level rise (SLR) is accelerating due to climate change [2], reliable projections of shoreline change on long (decadal to centennial) time scales are critical for coastal managers and decision makers [3,4]. SLR-driven shoreline recession occurs on time scales from decades to centuries as a result of the interaction between short- and long-term processes (e.g., wave action and SLR). Accurately integrating the SLR-driven erosion into more comprehensive shoreline change models is therefore necessary to improve our understanding and the predictability of long-term shoreline evolution in the context of climate change.

For the past 60 years, the Bruun [5] model (known as "Bruun Rule") has been the most widely used method to estimate long-term beach recession due to SLR, and its use in contemporary applications keeps growing (Figure 1). The core assumption of the Bruun Rule is that a beach maintains a constant elevation profile and migrates upwards and landwards under the influence of SLR, based on the concept of equilibrium beach profile adjustment, under a number of assumptions (outlined in Section 2). The validity of the Bruun Rule has been recently demonstrated in laboratory settings under certain conditions [6,7].

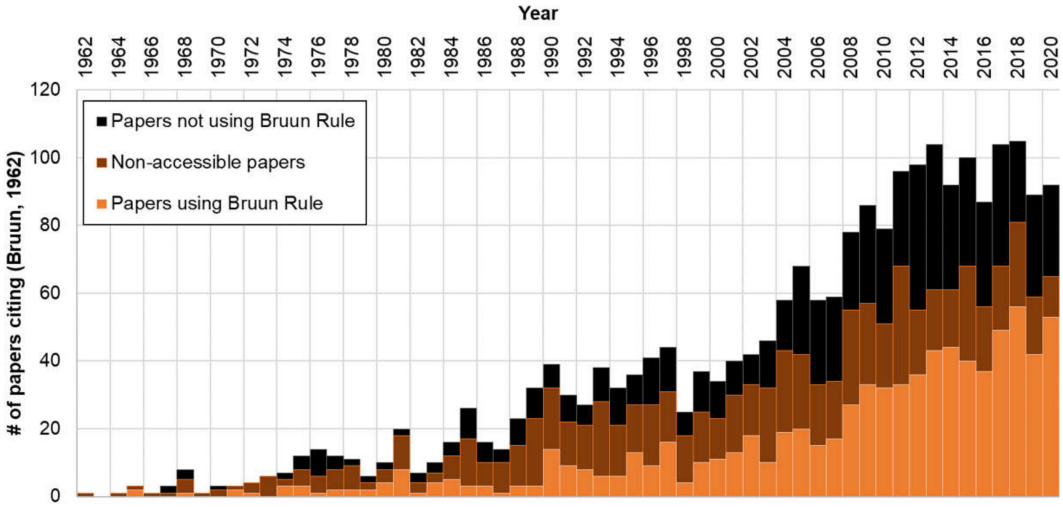

Figure 1. History of papers (per year) that cited Bruun [5] from 1962 to 2020, divided by: papers in which the Bruun Rule is employed (bright orange); non-accessible papers where the use of the Bruun Rule is uncertain (dark shaded orange); and papers citing Bruun [5] but not employing the Bruun Rule (black). Source: Google Scholar® search engine.

Bruun's model calculates shoreline recession explicitly as a function of SLR, and implicitly from the long-term effect of combined hydrodynamic processes (e.g., waves, tides, currents, etc.). To the authors' knowledge, the physical mechanisms of shoreline recession driven by the combination of waves and SLR has never been explicitly described.

In recent years, the development of equilibrium-based shoreline models (ESMs) enabled a skillful simulation of wave-driven shoreline change on cross-shore-transport-dominated coasts [8–12]. ESMs parameterize complex sediment transport processes and rely on shoreline data to calibrate free model parameters. Such parametrization allows for the modeling of shoreline behavior on time scales ranging from hours to decades at a low computational cost. These models are conceptually similar to the Bruun Rule in that the equilibrium beach profile adjusts to the forcing conditions. ESMs model the short-term dynamic beach response to incident wave conditions rather than adjustments due to sea-level change. During storms, the upper portions of the beach profile erode, and the sediment is deposited offshore in response to increased incident wave energy (see, e.g., Yates et al. [9]). When wave height declines, the sediment is moved back to the shore, driving the profile to its original shape. ESMs show skill in predicting erosion/accretion cycles on hourly (single storm) to yearly/decadal time scales (e.g., Splinter et al. [11], Yates et al. [9], Castelle et al. [13], Lemos et al. [14]).

Applying ESMs over long time scales, where sea-level rise becomes important, is a critical step toward more comprehensive long-term shoreline projections. The most widely used solution is to couple ESMs with the Bruun model [15–19]. However, so far, the effects of hydrodynamic processes implicitly modeled by the Bruun Rule have never been explored in detail, and applications coupling these processes disregarded the conceptual relationship between the two models. Therefore, coupling ESMs with SLR-driven recession models requires a re-examination of the basic hypotheses and underlying physical processes of these models to verify their compatibility, modify them if necessary and lay the foundations for further developments. Such a re-examination is particularly warranted given the accelerating SLR trajectories and the increasing reliance on the Bruun Rule (see Figure 1).

In this paper, we present a novel interpretation of the physical mechanism of SLR-driven erosion in the context of equilibrium beach theory, focusing on the interaction between short- and long-term drivers (i.e., wave action and SLR). We use the proposed concept (i) to provide a new perspective on the Bruun Rule's underlying physics and (ii) to analyze the integration of SLR-driven recession into ESMs. Finally, we identify and discuss potential future research avenues to extend the validity of integrated ESMs beyond the

limited set of conditions where the stand-alone Bruun Rule is applicable. The remainder of the paper includes a brief review of the Bruun model and the proposed interpretation of the generalized physical mechanism of SLR-driven shoreline recession, with an overview on ESMs and their potential role in quantifying SLR-driven shoreline change (Section 2); an analysis of the integrated SLR-driven recession and ESMs in a generalized case and under Bruun's assumptions (Section 3); and a model application to an idealized test case at the cross-shore-transport-dominated Truc Vert beach (Section 4). The results and implications for future improvements in shoreline modeling are discussed in Section 5. Conclusions are drawn in Section 6.

A list of symbols and notations (Table S1) and a list of acronyms (Table S2) used in this paper are included in the Supplementary Material. Appendix A provides mathematical insights on how the Bruun Rule can be expressed using the proposed conceptualization. Appendix B provides details on integrating ESMs and SLR-driven recession models with the dynamic feedbacks described in Section 3.2.

2. Sea-Level-Driven Recession and Equilibrium Shoreline Models

2.1. The Bruun Model

The Bruun Rule [5], which estimates a chronic beach recession due to SLR, is a one-dimensional representation of two-dimensional processes on a cross-shore beach profile. The model assumes that: (i) a theoretical equilibrium beach profile exists and is maintained over time; (ii) sediment volume is conserved cross-shore between the limits of the active beach profile (down to a so-called "depth of closure"); (iii) SLR always induces long-term shoreline retreat (as the beach profile migrates upward and landward with SLR in order to conserve sediment volume); and (iv) there is unlimited available sediment from the subaerial beach [20,21].

The theoretical equilibrium profile shape is determined by the local sediment and wave climate characteristics [22]. Therefore, the preservation of the equilibrium profile shape implies that the local wave climate characteristics remain roughly constant.

According to the Bruun model, under the assumptions listed above, the long-term beach profile responds to SLR with a landward and upward translation (Figure 2), producing a shoreline retreat (S_{Bruun}) given by:

$$S_{Bruun} = \frac{SLR}{\tan(\alpha)} \quad (1)$$

where tan(α) is the mean slope of the active beach profile between the offshore limit of sediment exchange (i.e., the depth of closure) and the stable emerged beach location (e.g., emerged berm, dune toe or dune crest). The depth of closure is determined by the local sediment size and the frequency of extreme waves over a given period of time, and thus depends on the local wave climate [23]. This last point highlights another strong link between the Bruun model and the wave climate. As the depth of closure depends on the time window observed and the respective distribution of extreme wave events [24], the assumption of a constant depth of closure implies a long-term stationarity of the wave climate.

The derivation of the original Bruun model was essentially based on an intuitive unification of physical beach characteristics and nearshore processes [21]. An implicit assumption of the Bruun model is that, in response to SLR, the sediment is redistributed over the profile by the long-term integrated effects of wave action [21]. This mechanism can be interpreted as the sea level setting a new non-equilibrium beach profile state, and the incident wave action mobilizing or relaxing the beach back toward equilibrium. Intuitively, if SLR occurred in the absence of sediment suspension and redistribution processes (e.g., waves), the shoreline regression would only result from the inundation of the landward profile (i.e., passive flooding [25]). This implies that the local wave climate must provide sufficient energy to mobilize sediment and reshape the profile quickly enough for the profile relaxation to keep pace with SLR [26]. Therefore, the shoreline recession modeled by

the Bruun Rule (Equation (1)) could be decomposed in two contributions: an instantaneous geometric shoreline retreat due to the flooding of the beach, and a long-term profile relaxation resulting from the cumulated action of nearshore hydrodynamic processes such as wave breaking. While the first is a well understood process (known as passive flooding), there is no explicit description of the physical mechanism driving the second contribution of the Bruunian response to SLR.

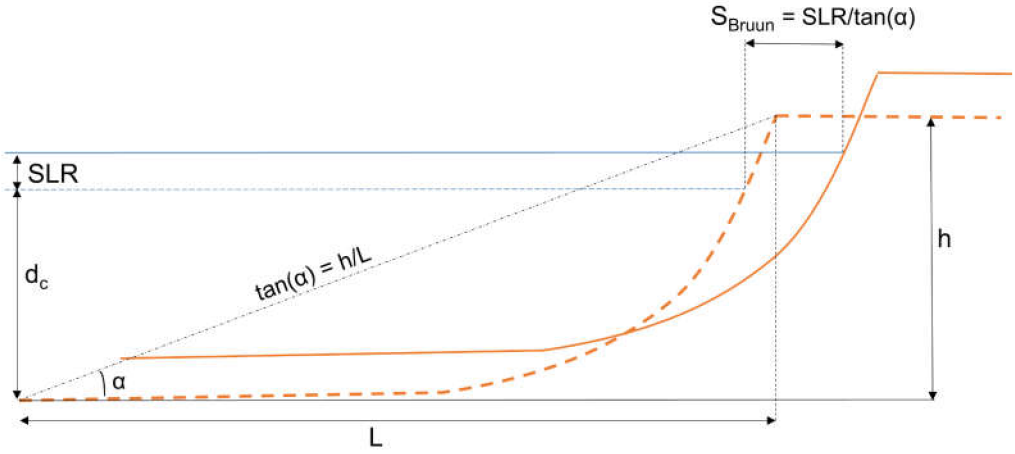

Figure 2. Schematic of the original Bruun model, where: SLR is the sea-level rise and S_{Bruun} the respective shoreline recession over the considered time lap; h and L are, respectively, the vertical and cross-shore extent of the active beach, delimited seaward by the depth of closure (d_c) and landward by the berm, dune toe or dune crest; and tan(α) is the average slope of the active beach profile.

Over the past two decades, several alternative interpretations of the model's underlying assumptions were provided to critically evaluate its validity as an independent predictive tool [27–30]. However, they did not investigate this second contribution. Instead, they highlighted processes omitted by the Bruun Rule, such as the influence of local geology and sediment supply [27], landward sediment transport, dune erosion and aeolian sediment transport, and proposed modified versions of the model to include these processes with additional terms [16,26,28]. The Bruun model was developed to account only for the contribution of SLR to long-term coastal recession and does not consider other possible contributions to erosion, such as the long-term variability of the wave climate [21]. Therefore, the applicability of the Bruun model alone is restricted to a limited range of coasts [21].

2.2. A physical Interpretation of the Beach Response to Sea-Level Rise

Consider an idealized equilibrium beach profile, where the shoreline (S) is defined as the instantaneous intersection of the beach profile and mean sea level (Figure 3a). Here, the foreshore is defined as the intertidal portion of beach between the mean high water (MHW) level and the mean low water (MLW) level (Figure 3). With a stable mean sea level, the local wave climate produces seasonal fluctuations in the cross-shore beach profile around its theoretical equilibrium position. A rise in sea level floods the foreshore (Figure 3b), leading to a shoreline recession (Passive Flooding, S_{PF}) proportional to the average foreshore slope, as follows:

$$S_{PF} = \frac{SLR}{\tan(\beta)} \quad (2)$$

where tan(β) is the mean foreshore slope. The shoreline recession due to passive flooding is purely geometric: it is the simple result of the change of the reference shoreline position (e.g., MSL), and occurs in the absence of sediment transport [25]. However, with respect to the new MSL (MSL' in Figure 3b), the beach slope across the profile is generally higher when the profile is concave (Figure 3b), as is the case for the majority of real beaches. A generally

steeper (more accreted) profile is, on average, more balanced with low energy waves and less balanced with high energy waves [31]. Hence, the elevated mean sea-level position (MSL') brings the "beach–wave climate" system into a disequilibrium state where the current wave conditions are larger than in the equilibrium state. Consequently, continuous wave action tends to reshape the beach profile toward its equilibrium shape (Figure 3c), driving a further landward displacement of the shoreline position (Wave Reshaping, S_{WR}). Recall that the beach profile in equilibrium with MSL' (Figure 3c) represents the mean position of the seasonal profile fluctuations. Therefore, depending on the energy provided by the incident wave conditions after a rise in sea level, the resulting, time-dependent effect of wave reshaping (here called d S_{WR}) may not immediately reach S_{WR} (Figure 3c), but would be gradually achieved with the cumulative wave action. In this mechanism, S_{PF} occurs simultaneously with SLR, while the associated S_{WR} develops on the time scale of several wave events.

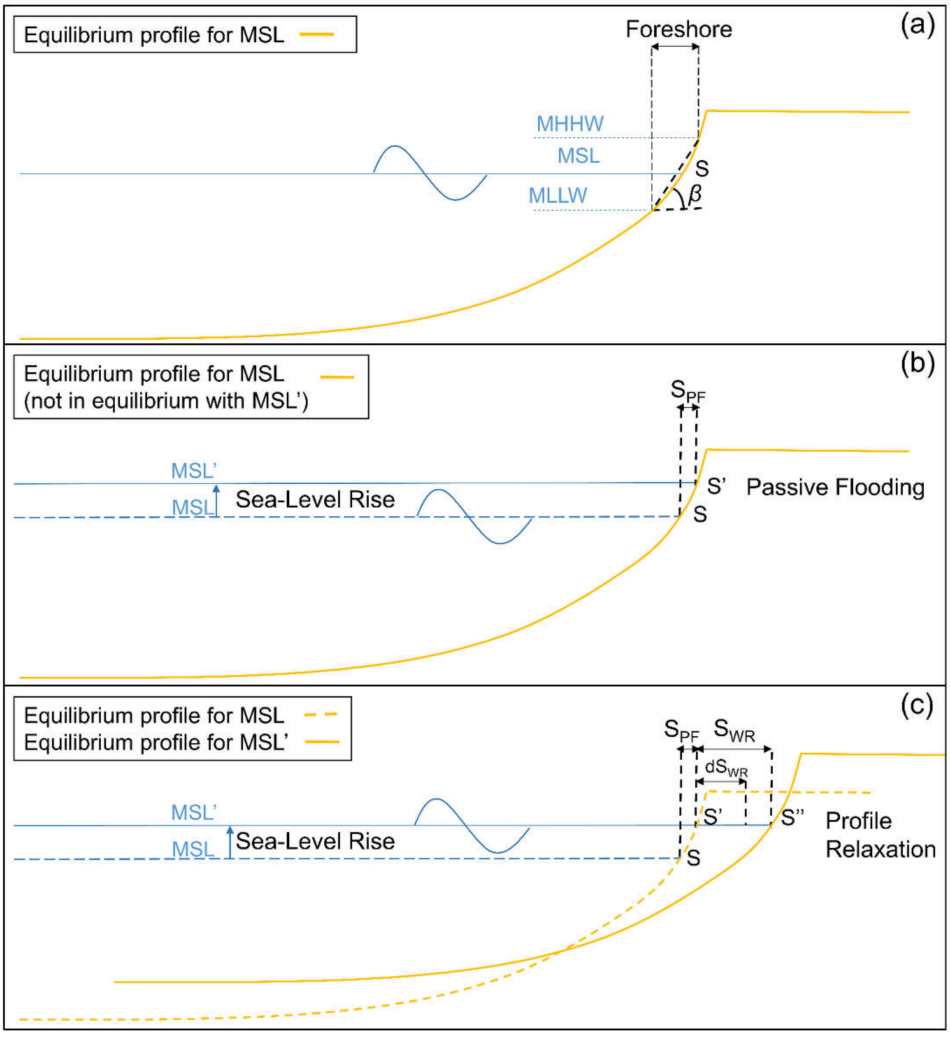

Figure 3. Scheme of the SLR-induced beach recession's physical conceptualization: (**a**) theoretical equilibrium profile for the given mean sea-level, tide and wave conditions; (**b**) passive flooding of the profile for a given rise in sea level; (**c**) profile relaxation driven by wave action in response to the disequilibrium between wave climate and the profile in panel (**b**) with the new mean sea level.

When the Bruun Rule assumptions (Section 2.1) are satisfied, namely the assumption of stationary long-term wave climate and constant SLR rate, over periods associating no trends in wave climate (e.g., $dT \geq$ O(year)), the mean rates of passive flooding and wave reshaping effects are constant (see Appendix A for more details). Therefore, under these

specific conditions, on the time scale of dT, the Bruun Rule can be expressed in terms of cumulated passive flooding and wave reshaping effects, as follows:

$$S_{Bruun} = \frac{SLR}{tan(\alpha)} = S_{PF} + S_{WR} \quad (3)$$

Differently from the passive-flooding component (S_{PF}), the wave reshaping term (S_{WR}) results from sediment transport processes. In fact, S_{WR} is the result of the change in wave-energy efficiency on sediment transport over a fixed amount of time, dt, due to the disequilibrium introduced by the sea-level change. Thus, quantifying S_{WR} requires the evaluation of the disequilibrium increase induced by SLR, and the functional correspondence between shoreline response and disequilibrium state. This is discussed in the next two subsections.

2.3. Disequilibrium and Beach Profile Relaxation in Equilibrium Shoreline Models

Equilibrium shoreline models (ESMs) assume the existence of an equilibrium beach profile and rely on the concept of disequilibrium between the current beach state and the current wave conditions [31]. A general ESM schematization is given by:

$$\frac{dS}{dt} = k^{+/-} F \, \Delta D \quad (4)$$

where F is the incident wave thrust function, ΔD the disequilibrium state, and $k^{+/-}$ a model free response rate parameter that has different values for accretion ($\Delta D > 0$) and erosion ($\Delta D < 0$) events, and can assume different physical meanings based on the formulation of F and ΔD (e.g., equilibrium time scale, or wave power efficiency). The time-varying disequilibrium condition ΔD can be defined in reference to the current beach profile position [8,9,12,15,17,32,33] or to the wave history [10,11,34]. Typical expressions of disequilibrium conditions based on shoreline position (ΔD_1) and wave history (ΔD_2) are shown in Equations (5) and (7), respectively:

$$\Delta D_1 = E_{eq}(S) - E \quad (5)$$

where E is the incident wave energy, S is the current shoreline position and E_{eq} is the wave energy in equilibrium with S and the beach profile, i.e., the wave energy that would cause no change to the current shoreline position S, defined, for instance, by a linear relationship:

$$E_{eq} = aS + b \quad (6)$$

with a and b being two empirical parameters, as in Yates et al. [9];

$$\Delta D_2 = \left(\frac{H_s}{T_p}\right) - \left(\frac{H_s}{T_p}\right)_{eq} \quad (7)$$

where H_s is the incident significant wave height, T_p is the peak wave period and $(H_s/T_p)_{eq}$ is an equilibrium wave condition defined as function of the past wave conditions (e.g., a weighted average of the past H_s/T_p over a period Φ, calibrated for the site of application; see, e.g., Splinter et al. [11]).

Depending on the approach, ΔD can thus be quantified in different ways, using either equilibrium wave energy or wave steepness, as in Equations (5) and (6), respectively. Each approach to evaluate ΔD (and F) is associated to a different physical interpretation to the k parameter [35]. However, regardless of the way it is defined, the disequilibrium state ΔD at a given time expresses the direction of shoreline response as well as the efficiency of the incoming wave in shaping the profile toward its theoretical equilibrium state.

2.4. Sea-Level-Rise-Driven Disequilibrium within ESMs

In the context of SLR, the explicit relationship between the disequilibrium state of the beach (ΔD) and the wave-driven shoreline change provided by ESMs can be used to quantify the wave reshaping effect (dS_{WR}) responding to the sea-level-induced disequilibrium.

For instance, consider an ESM based on the current shoreline position (Equation (5)), where the equilibrium wave energy (E_{eq}) is expressed by Equation (6). An increase in MSL (dMSL) induces passive flooding (dS_{PF}), corresponding to a landward shift of the reference shoreline (Figure 3b), i.e., a smaller S value. Recall that this shift represents only a translation of the reference system, with no morphologic change to the beach profile. The second consequence of SLR, observed in Figure 3b, is a general increase in the bottom slope relative to the local wave climate propagating over the new MSL. In morphologic terms, this steeper beach profile is no longer in equilibrium for the mean wave climate at the site of interest. In particular, the steeper beach profile is closer to the equilibrium profile for low energy wave conditions, and farther to the equilibrium profile for high energy wave conditions [31]. If the mean wave climate does not change, wave events are more likely to result in an overall (erosive) disequilibrium of the "beach–wave climate" system (Figure 3c). As the equilibrium condition is defined in terms of wave energy (E), the SLR-induced disequilibrium can be expressed as a decrease in equilibrium wave energy ($dE_{eq,SLR} < 0$), and can be injected in Equation (6):

$$E_{eq} = aS + b + dE_{eq,SLR} \tag{8}$$

This indicates that, for a given shoreline position (S), less wave energy is required to erode the beach and restore the equilibrium. Or, alternatively, for a given wave condition, the mean erosive efficiency of waves is increased, which likely results from an increased bottom slope across the beach profile due to SLR and wave breaking tending to occur closer to the shore.

Further insights on $dE_{eq,SLR}$ are provided in Section 3.2.

3. Integrating Sea-Level Rise in Equilibrium Shoreline Models

SLR-driven erosion can be integrated with ESMs using different methods. In turn, the ESMs' response to SLR can be different depending on how sea-level change is implemented in the model and whether the applied disequilibrium condition is influenced by the sea level. Below, we analyze approaches where wave-driven shoreline change and the effects of SLR are evaluated separately and combined linearly (Section 3.1), and approaches where the ESM's disequilibrium condition interacts dynamically with the effects of SLR (Section 3.2).

3.1. Linear Combinations of SLR Effects and ESMs

If the ESM's equilibrium formulation is based on wave history (Equation (7)), the impact of SLR can be integrated by linearly combining the ESM with passive flooding and wave reshaping models at each time step, and the differential equation for shoreline change reads:

$$dS = \left(k^{+/-} F\, \Delta D_2\right) dt + dS_{PF} + dS_{WR} \tag{9}$$

ESMs with disequilibrium conditions that are a function of shoreline position (e.g., based on Yates et al. [9], as in Equation (5)) can be sensitive to sea-level change or to the permanent flooding dS_{PF} that follows. For this type of ESMs, the shoreline changes caused by short-term (ST) and long-term (LT) processes can be treated as independent components to avoid spurious feedbacks between the ESM and the SLR impact model:

$$dS_{ST} = k^{+/-} F \left(E_{eq}(S_{ST}) - E\right) dt \tag{10}$$

$$dS_{LT} = dS_{PF} + dS_{WR} \tag{11}$$

$$dS = dS_{ST} + dS_{LT} \tag{12}$$

so that the ESM and SLR effects ($S_{PF} + S_{WR}$) are computed independently over the simulated period and then simply added. In such approaches, the equilibrium energy term in Equation (5) is a function of the sole current shoreline position driven by the wave action in the absence of SLR ($E_{eq} = E_{eq}(S)$).

For applications where Bruun's assumptions are satisfied, the SLR-driven shoreline retreat in Equation (9) and Equations (10)–(12) can be given by the Bruun model (Equation (3)). Such linear combination between ESMs and the Bruun model has been done in several previous applications (see, e.g., D'Anna et al. [18,19], Robinet et al. [36] and Vitousek et al. [17]). However, these studies did not explicitly acknowledge the physical mechanisms underlying the Bruun model (i.e., $S_{PF} + S_{WR}$).

3.2. SLR Effects and ESMs with Dynamic Interactions

Below, we illustrate an alternative to the approach described by Equations (10)–(12), in which short- and long-term shoreline change are resolved in the same equation system at each time step (dt) for ESMs with disequilibrium conditions that are a function of shoreline position (e.g., Equation (5)), thereby enabling feedbacks between the modeled processes. Here, the wave reshaping (dS_{WR}) is explicitly computed at each time step within the ESM as a response to passive flooding (and thus to SLR). If SLR is applied at a given time step, the consequent dS_{PF} is added on the short-term to the ESM (Equation (4)), accounting for the shoreline retreat induced by passive flooding. If the equilibrium condition is expressed as $E_{eq}\ (S) = aS + b$ (as per Yates et al. [9]), then the first (geometric) effect of passive flooding results in a disequilibrium change $dE_{eq,SLR}$, which affects the wave-driven shoreline response and results in the wave reshaping (dS_{WR}) effect, as explained in Section 2.4. Quantifying $dE_{eq,SLR}$, i.e., the change in equilibrium wave energy due to SLR, is not straightforward. To our knowledge, the literature does not provide a physical expression of the increase in wave-driven erosion efficiency as a function of SLR. Therefore, to go one step further in the quantification of this complex interaction, we make the reasonable (though approximate) assumption that the increase in wave efficiency ($dE_{eq,SLR}$) has the same magnitude as the apparent increase in wave energy associated with the passive flooding shift (i.e., $dE_{eq,SLR} = -a\ dS_{PF}$, which is further explored in Appendix B). Such assumption is realistic, as it translates that the steepening of the beach profile relative to the risen MSL is equivalent to the effect of an apparent accretion event that wave reshaping tends to reverse. Hence, for a given wave energy, additional erosion must occur (resulting from an elevated SLR), and, consequently, the magnitude of this wave-efficiency-driven erosion (dS_{WR}) is the same as dS_{PF}. We further discuss the development of this assumption and its consistency with the Bruun Rule in Appendix B. The assumption above is based on intuitive physical considerations and is used in the present paper for demonstrational purposes in the following sections. We discuss alternative methods to estimate $dE_{eq,SLR}$ that do not rely on this assumption in Section 5. Here, where the disequilibrium condition is based on the shoreline position, the disequilibrium change caused by SLR ($dE_{eq,SLR}$), which produces dS_{WR}, can be expressed adopting the assumption above and injected into Equation (5), obtaining:

$$E^*_{eq}\left(S,\ dE_{eq,\ SLR}\right) = aS + b + dE_{eq,\ SLR} \tag{13}$$

$$\Delta D^*_1 = E^*_{eq}\left(S,\ dE_{eq,\ SLR}\right) - E \tag{14}$$

where the (*) symbol indicates that the disequilibrium condition responds to short-term changes in the shoreline position accounting for the geometric changes in the reference shoreline position due to passive flooding. Recall that although the additional SLR-induced disequilibrium is expressed as a function of dS_{PF}, the resulting dS_{WR} is of a different nature (Section 2.2). In response to the altered equilibrium owing to SLR, the model captures a time-dependent, wave-driven erosion process at each modeled time step to profile reshaping

(dS_{WR}). In this approach, the instantaneous adjustment to SLR is included by adding the sole dS_{PF} term to the ESM and using the equilibrium condition in Equation (13):

$$dS = k^{+/-} F\left(E^*_{eq} - E\right)dt + dS_{PF} \quad (15)$$

Approaches that modified the equilibrium condition of ESMs to integrate additional physical processes have been previously proposed in the literature. For example, Jaramillo et al. [37] introduced shoreline trends associated with long-term sources and sinks of sediment (e.g., gradients in longshore sediment transport or beach nourishments), using an empirical linear term. Other approaches that modified the ESM's disequilibrium condition were applied under the validity of Bruun's assumptions, although they were based on Bruun-like [15,38] or empirical terms [8,33] and did not identify separate contributions to SLR-driven erosion, such as S_{PF} and S_{WR}.

Figure 4 illustrates the behavior of a model using the approach proposed in Equation (15) in response to a perturbation of MSL, in a simple idealized setup. Equation (15) is forced with constant wave forcing F (where $F = E^{0.5}$ and $E = H_s{}^2/16$) and a stepwise increase in sea level of 30 cm (Figure 4a). In this example, we apply realistic values of the model parameters a, b, k^+ and k^- (see Table 1), and a mean wave height H_s of 2.5 m, which are derived from the test case described in Section 4.1. Then, we repeated the application increasing and decreasing the mean wave height by 50% (i.e., 3.75 m and 1.25 m, respectively).

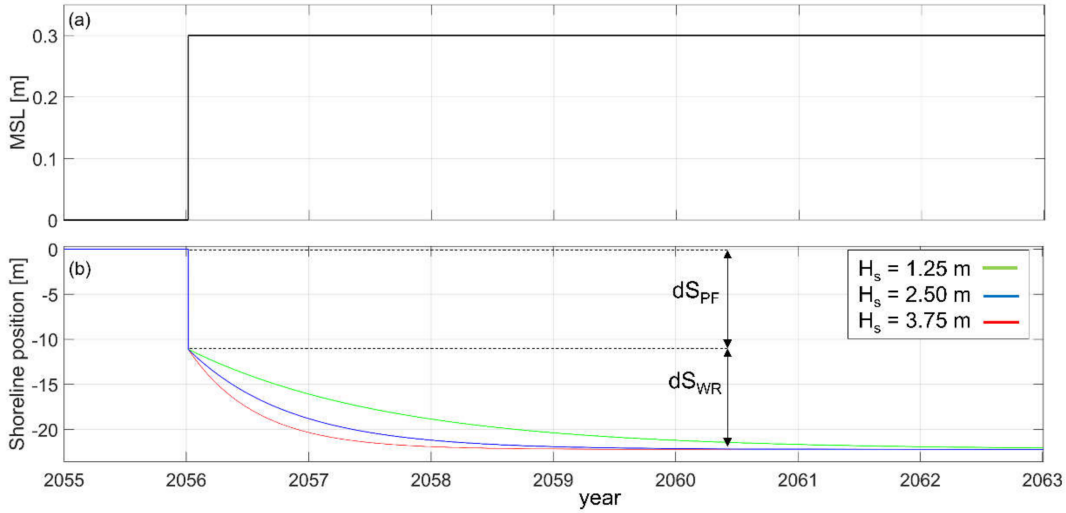

Figure 4. Application of the approach proposed in Equation (15), using constant wave energy and a 30 cm instantaneous sea-level rise. (**a**) Mean sea-level time series used in the application; (**b**) shoreline response showing the instantaneous passive flooding and the progressive effect of wave reshaping for a constant mean incident wave height of 1.25 m (green line), 2.50 m (blue line) and 3.75 m (red line).

Table 1. Simulation setup information including the governing equation, disequilibrium approach, SLR approach and calibrated model free parameters. The (*) symbol indicates that the feedback between the models is enabled.

Simulation	Model	ΔD	SLR-Driven Model	k^+	k^-	a	b	Φ
S14 NoSLR	Equation (4)	ΔD_2	-	1.01^{-8} $[ms^{-1}(W/m)^{-0.5}]$	4.40^{-8} $[ms^{-1}(W/m)^{-0.5}]$	-	-	1187 [days]
S14 + B	Equation (9)	ΔD_2	Bruun					
Y09 NoSLR	Equation (4)	ΔD_1	-	0.54 $[ms^{-1}/m]$	0.68 $[ms^{-1}/m]$	-0.01 $[m^2/m]$	0.55 $[m^2]$	-
Y09 + B	Equations (10)–(12)	ΔD_1	Bruun					
(Y09 + PF)*	Equation (15)	$\Delta D *_1$	PF					

After a first period of stable shoreline position, in equilibrium with the applied constant wave energy, Figure 4b shows the two separate effects of passive flooding and wave reshaping, i.e., an instantaneous retreat corresponding to the immediate passive flooding induced by the stepwise SLR, followed by a gradual erosion produced by the wave action to relax the beach profile into a new equilibrium condition. Such modeled behavior shows the same characteristics of shoreline response to step-wise SLR observed in laboratory settings under stationary wave conditions [6]. In response to the change in sea level, the relaxation time of the beach profile toward the equilibrium position associated with different constant wave conditions would have been shorter (longer) for more (less) energetic waves (Figure 4b). This means that for a fast-changing sea level and persistent low-energy wave conditions, the instantaneous passive flooding and the slow development of the wave reshaping effect can be more easily isolated. Moreover, such conditions may not allow the full relaxation of the beach profile (and therefore dS_{WR}) until the occurrence of a high-energy wave event (e.g., storm).

4. Model Application

4.1. Test Case

The following application aims at showing that when the assumptions underpinning the Bruun model (Section 2.1) are satisfied, the proposed mechanism explains the physics of the Bruun model shoreline retreat. We apply the variants of the combined SLR- and wave-driven shoreline change developed above, in Equations (9)–(15), to model 88 years of shoreline change at Truc Vert beach, in southwest France (Figure 5a,b), in an idealized setup that satisfies the main Bruun model's assumptions (i.e., cross-shore transport only, conservation of a long-term trend in wave energy and constant SLR rate). The following test case is intended as a proof-of-concept study rather than a site-specific hazard assessment. Hence, the results are generalizable to cross-shore-dominated beaches around the world where Bruun's conditions apply.

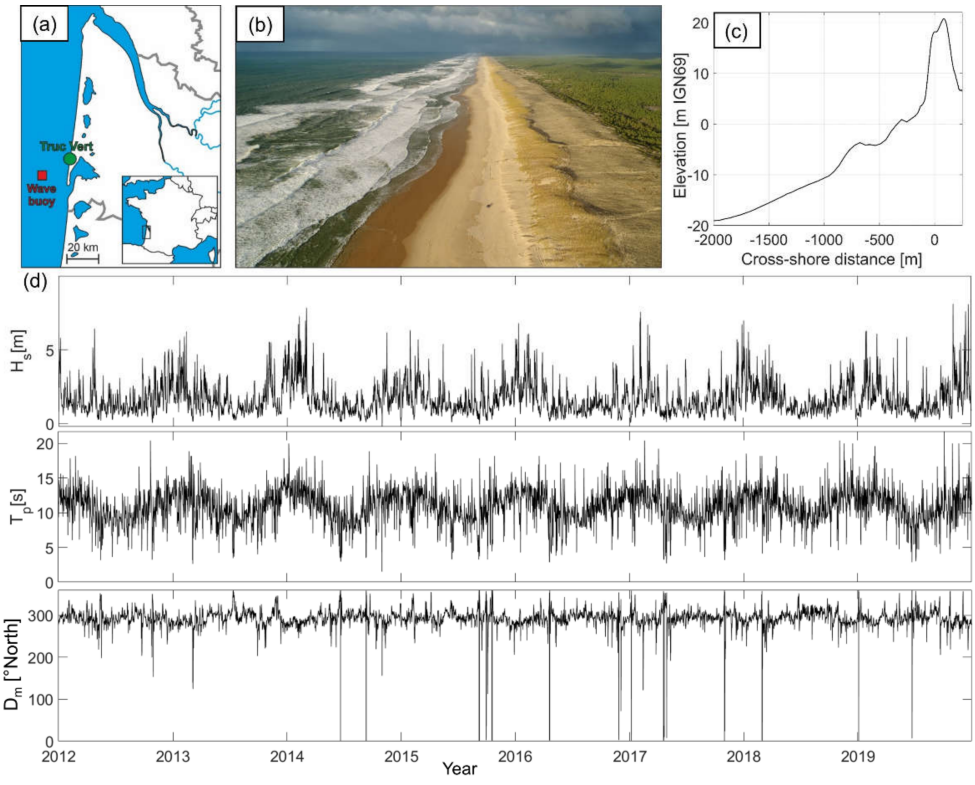

Figure 5. (**a**) Truc Vert beach location (green) and wave data location corresponding to the wave buoy (red); (**b**) photo of Truc Vert beach (photo by V. Marieu); (**c**) alongshore averaged beach profile; (**d**) 2012 to 2019 time series of H_s, T_p and D_m.

Shoreline change at Truc Vert is essentially driven by cross-shore processes (see Castelle et al. [13], Robinet et al. [39] and D'Anna et al. [19] for more details). ESMs were found to reproduce the shoreline evolution over a decadal time scale at Truc Vert with very good results, using equilibrium based on wave history [11,13,18], but also based on the shoreline position [13,19], i.e., using Equations (6) and (5), respectively. The shoreline variability at Truc Vert beach is characterized by seasonal and interannual cycles with an amplitude of tens of meters, making this site a good benchmark for ESMs.

Historical wave conditions (significant wave height H_s, peak period T_p, mean direction D_m) over the period between 01 January 2012 and 31 December 2019, associated with no long-term shoreline trend on the same period, are extracted from the NORGAS-UG hindcast (Ifremer-LOPS-SHOM) at the Cap Ferret buoy located offshore, in a ~50-m depth (Figure 5a). A synthetic wave time series, constructed by replicating the historical (2012–2019) time series end-to-end over 80 years, is then used to force the model from 01 January 2012 to 31 December 2099. Such a simplified approach is sufficient to compare different models under a periodic wave climate, which is required for the application of the Bruun model. Breaking wave conditions are computed using the direct formula of Larson et al. [40], which is derived from a simplified solution of the combined wave energy flux conservation equation and Snell's law in the assumption of shore-parallel bathymetry contours. SLR rates were evaluated at this site using SROCC projections [2] for the high emission RCP 8.5 scenario, considering the regional fingerprints of sea-level change contributors, over the simulation period (Figure 6). This corresponds to a SLR rate of ~1 cm/year by the mid-21st century [2,41]. The main characteristics of the active beach profile (Figure 5c) are estimated using a 2-m resolution topo-bathymetry and a high-resolution digital elevation model described in D'Anna et al. [18]. The mean profile slope ($\tan(\alpha)$) required by the Bruun model is calculated using the beach profile (Figure 5c) between the dune toe and the depth of closure obtained from the Hallermeier formula (see Equation (3) of Hallermeier [23]). The latter computes the yearly depth of closure as a function of the wave height exceeded for 12 h in a year ($H_{0.137\%}$) and the corresponding wave period. Given that this calculation depends on the period of the wave time series over which extreme wave conditions are extracted, we applied the Hallermeier formula to each year of the available wave data and adopted the median of the resulting values (~14 m). The resulting mean profile slope is $\tan(\alpha) = 0.014$. The time average foreshore slope $\tan(\beta)$ is estimated from the portion of beach profile between the MHW (+1.39 m Above Mean Sea Level) and MLW (−1.54 m Above Mean Sea Level) using 84 topographic surveys between 2016 and 2019, with $\tan(\beta) = 0.026$.

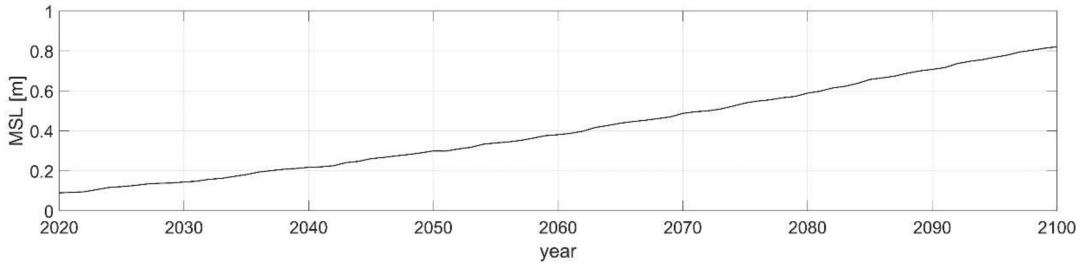

Figure 6. Future mean sea level time series estimated at Truc Vert using median SROCC sea-level rise projections in the RCP8.5 scenario.

ESMs are run at a 1-h time step using the two different disequilibrium approaches described in Section 3. In the first approach (hereafter Y09, referring to the Yates et al. [9]-like model) the disequilibrium condition is based on a prior shoreline position (Equation (5), with $E_{eq} = aS + b$, while the square root of wave energy at breaking is used as forcing (F), in line with models based on this type of disequilibrium condition [9,12,14,42,43]. The second approach (hereafter S14, referring to the Splinter et al. [11]-like model) adopts a disequilibrium condition based on the offshore wave history (Equation (7)), with $(H_{o,s}/T_p)_{eq}$ defined

as the weighted average of $H_{o,s}/T_p$ over the previous Φ days, and the square root of wave power at breaking as forcing, similarly to models using this type of approach [10,11,18,36]. For each approach, the ESM $k^{+/-}$ and respective parameters (a and b for Y09, and Φ for S14) are calibrated using the Simulated Annealing optimization technique [44] described in D'Anna et al. [18] on Equation (4). Compared to D'Anna et al. [18], who used the Truc Vert shoreline data up to 2017, the time series of mean shoreline position estimated here with topographic surveys is extended to the end of 2019 [45]. The calibration is performed over the period 01 January 2012–31 December 2019, which shows no long-term shoreline trend (Figure 7a). For the purpose of the present idealized case application, we assumed that no SLR occurs over the calibration period, so that the models reproduce the shoreline evolution as the only response to the wave climate, with no long-term trend. The optimized parameters are reported in Table 1. The resulting Y09 and S14 models produce a Root-Mean-Square-Error of 4.68m and 6.99m, respectively, and a coefficient of determination R^2 of 0.83 and 0.62, respectively. Over the calibration period, Y09 captures the interannual shoreline variability better, producing a higher R^2. However, both models visually demonstrate good skill and capture the overall shoreline behavior (Figure 7a). A preliminary simulation over the period 2012–2099 with no SLR is performed for each model to verify that the ESM does not produce any long-term shoreline trend in the absence of SLR ('Y09 NoSLR' and 'S14 NoSLR' in Figure 7b and Table 1).

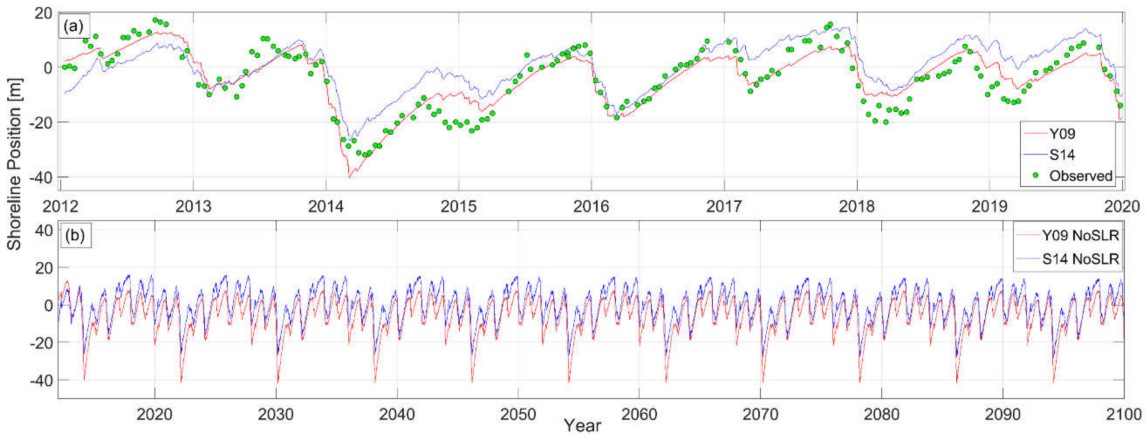

Figure 7. (**a**) Shoreline time series over the period 2012–2019. The red and blue lines represent the modeled shoreline obtained using Y09 and S14, respectively, and the green dots represent the mean shoreline position estimated from topographic surveys. (**b**) Modeled shoreline time series from 01 January 2012 to 31 December 2099 with no SLR.

4.2. Integration of SLR Impact Model into ESMs

Three simulations were run, coupling first S14 and Y09 with the Bruun model (B) and no feedback (Equations (9) and (12), respectively), and then the Y09 with a "passive flooding" (PF) model feeding back into the equilibrium condition (Equation (15). As the configuration of the applications satisfies the main Bruun model assumptions (no long-term variability of the wave climate, absence of processes other than SLR inducing shoreline trends, no short-term sea level fluctuations), the simulation results are expected to be consistent with the Bruun model and reproduce the cumulated effects of S_{PF} and S_{WR}.

4.3. Results

Figure 8a shows that the simulated shoreline positions produced with the model configurations (Y09 + B) and (S14 + B) are consistent and in line with the trend estimated by the Bruun model alone (black line). These results show that, in the absence of feedback between the ESM and the SLR impact model (i.e., the disequilibrium approach is independent from the SLR-induced shoreline change), the ESM reproduces the short-term shoreline fluctuations and the Bruun model reproduces the long-term S_{PF} and S_{WR} contributions.

The combined (Y09 + PF)* models reproduce the effects of SLR on the shoreline consistently with the individual Bruun model (Equation (1)). This suggests that introducing dS_{PF} (PF model) into the ESM, the consequent disequilibrium increase ($dE_{eq,SLR}$), which reproduces the dS_{WR}, explains the Bruun model's results (Figure 8b). As SLR is applied to (Y09 + PF)* at each time step, the relative passive flood dS_{PF} and the resulting wave reshaping (dS_{WR}) are infinitesimal compared to the sole wave-driven shoreline change. The latter is such that the difference between the (Y09 + PF)* and (Y09 + B) results is minimal (Figure 8a,b and Table 2). However, the difference between the two model results (Figure 8c) shows seasonal fluctuations, with larger magnitudes in the summer (low wave energy) and smaller magnitudes in the winters (high energy). In fact, in the (Y09 + PF)* model the wave reshaping (dS_{WR}) produced in response to SLR occurs at a slower rate during low energy periods (summer) and a higher rate during high energy periods (winters) (see Section 2.2, Figure 3c) compared to the average rate produced by the Bruun Rule (Appendix A). Such seasonal behavior highlights the role of wave energy trends (in this case seasonal) on the magnitude of the modeled wave reshaping component (dS_{WR}). Recall that this is a theoretical scenario, in which all Bruun's assumptions are satisfied. In reality, such conditions are not granted, and other processes, such as variability in wave climate, may dominate the evolution of the beach when combined with SLR [46]. Applications of the (Y09 + PF)* to these cases are expected to capture interactions between waves and SLR and produce results that diverge from the Bruun model application.

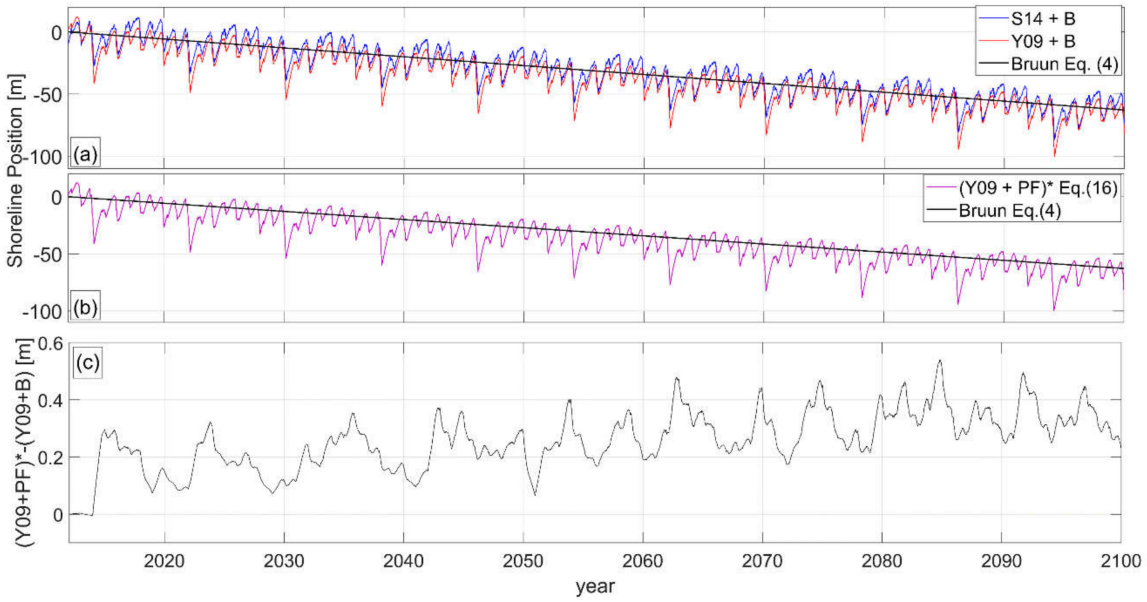

Figure 8. (**a**) Model Results for the Y09 and S14 approaches integrated with the Bruun model with no feedback (red and blue curve, respectively), using Equations (9) and (12), respectively, and the sole Bruun model (black curve); (**b**) Model results for the Y09 approach integrated with the PF with feedback (red curve), using Equation (15), and the sole Bruun model (black curve); (**c**) difference between the (Y09 + PF)* and (Y09 + B) model results. The negative and positive dS correspond to erosion and accretion, respectively.

Table 2. Eight-year averaged shoreline position at 2100, and minimum, maximum and standard deviation of the shoreline position over the last 8 simulated years, for (Y09 + PF)*, (Y09 + B) and the Bruun Rule.

	Shoreline Position		
Model	**8-Year Mean from at 2100 [m]**	**[min; Max] Over Last 8-Years [m]**	**σ Over Last 8-Years [m]**
(Y09 + PF)*	−58	[−41; −100]	8.7
(Y09 + B)	−58.5	[−41; −100]	8.7
Bruun	−55	[−55; −55]	0

5. Discussion

5.1. Bruun Rule Interpretation

The idealized model applications suggest that when the Bruun Rule's assumptions are satisfied, the results obtained with (Y09 + PF)* and the Bruun Rule are consistent. This indicates that under these specific conditions the physics of the Bruun model can be explained by our proposed interpretation (i.e., $dS_{PF} + dS_{WR}$). The latter does not aim to validate or encourage the use of the Bruun model, but highlights that, in a geomorphology context where the Bruun's assumptions are tenable, our proposed mechanism provides a physical explanation for the magnitudes and time scales of the Bruun Rule's shoreline recession. When the conditions for the application of the Bruun model are not met (i.e., short time scale, long-term variability of wave climate, presence of sources or sinks of sediment, limited accommodation space, etc.), the Bruun Rule is expected to fail [27,47–49], while, as long as the dS_{WR} component is resolved at the time scale of wave events, the physical mechanism proposed here remains valid.

For instance, current rates of SLR are in the order of mm/year and can increase to cm/year by mid-century (SROCC projections [2]). Therefore, SLR can be considered as a quasi-static process when analyzing shoreline change by tide- and wave-induced processes. However, our concept can potentially be applied to any time scale, down to a single wave event (hours), as it captures the contribution to dS_{WR} of each wave event in response to changes in MSL. Although on time scales shorter than years the recession due to SLR (i.e., dS_{PF} and dS_{WR}) is infinitesimal compared to the wave-driven shoreline change, other irregular processes acting on these time scales (e.g., wave climate variability, longshore sediment transport, etc.) and/or short-term sea-level changes (e.g., storm surges) may affect the beach equilibrium state and, in turn, the instantaneous dS_{PF} and cumulative dS_{WR}.

Resolving the passive flooding effects on the time scale of wave events (hours) also allows us to model the shoreline response to the lowering sea level, accounting for the varying efficiency of erosion and accretion processes. In fact, lowering sea level would reduce the flooded area (inducing a first seaward shoreline migration), while the lowered MSL associates a reduced slope across the profile (that appears more eroded), which is more balanced with high energy waves and less balanced with low energy waves [31]. Thus, the lowering sea level drives the "beach–wave climate" system into a disequilibrium state where the wave-driven-erosion efficiency is reduced. Instead, although the Bruun model can be applied in such case, the underlying physical assumptions are not designed for lowering sea levels [20,21].

5.2. Integrating ESMs and SLR-Driven Shoreline Models

Based on the proposed physical interpretation of the SLR-driven shoreline response, our analytical discussion identifies multiple generalized approaches to integrate SLR effects into ESMs where passive flooding and the wave reshaping effect are explicitly resolved. The analysis shows that two approaches can be adopted to include the shoreline relaxation that follows passive flooding (Figure 3c, Sections 2.2 and 2.4) into ESMs. If the ESM disequilibrium condition is based on wave history (e.g., Equation (7)), the integration of dS_{PF} does not alter the disequilibrium, so that the term dS_{WR} should be computed separately and added. Instead, ESMs relying on the shoreline position to define the disequilibrium condition may require or not the additional dS_{WR} term, depending on whether feedbacks between model equations are enabled or not. In the first two instances (ESMs based on wave history or shoreline position with no feedback) a specific function that quantifies dS_{WR} in response to SLR is required. Instead, when feedback is allowed within ESMs based on previous shoreline positions (Equation (15), the model produces dS_{WR}, provided that a relationship between dS_{PF} (or SLR) and $dE_{eq,SLR}$ is assigned. Here, particular attention must be paid to the potential role of wave energy trends in the modeling of dS_{WR}.

It must be noted that using the Bruun model with ESMs [17,19,36,38] assumes a constant active profile, which implicitly assumes a stationary wave climate. Therefore, applications to regions subject to statistically significant wave climate changes must be

performed with care. The available global studies (0.5° to 1.5° spatial resolution) indicate significant changes in wave climate offshore (~200 m depth) of ~50% of the world's coastline over the next century (COWCLIP, [50]), suggesting that significant nearshore wave changes may be expected in some localized areas. In addition, when addressing future shoreline variability (rather than overall trends), changes in the seasonal and interannual variability of the wave climate as well as storminess could modify the shoreline behavior [51,52], and should be accounted. Coupling SLR and ESM models with feedback resolves all SLR-induced shoreline change components on the same short time scale, reproducing the wave-event by wave-event response of the shoreline to passive flooding and capturing the joint effects of SLR with possible changes in the wave energy distribution.

5.3. Applications of Integrated Shoreline Models and Uncertainties

While ESMs are generally applicable to cross-shore-transport-dominated open beaches, the quantity, frequency and accuracy of the available shoreline data at a given site are a potential source of model uncertainty [18,19,52,53]. In real case applications of ESMs (with or without SLR-driven erosion component), such uncertainties can be empirically quantified and introduced in the frame of probabilistic shoreline predictions [18,19,54–56]. Here, however, we performed an idealized model application to compare the behavior of different model combinations, and the evaluation of model uncertainty, as well as a full validation of the wave-driven models, is outside the scope of this work.

Our idealized model application is forced using a synthetic wave time series obtained by replicating 8 years of wave hindcast data. Although this is a simplistic approach, such wave series ensures that the Bruun's assumption of steady wave climate is satisfied. In real case applications, where the Bruun's assumptions are not necessarily satisfied, the model should be forced with realistic wave time series. Given the key role of short- and long-term variability of the incident wave energy in equilibrium-based models (integrated or not), uncertainties on the inherent variability of the wave climate should be considered [19,35]. The latter can be addressed by performing ensemble simulations using a large number of different plausible wave series generated, for instance, with statistical methods [35,57,58]. However, in this proof-of-concept study we aim to analyze the behavior of integrated models in an idealized context where Bruun's assumptions are satisfied, and the construction of a more realistic synthetic wave time series is beyond our scope.

The SLR-induced shoreline change component is very sensitive to the slope used into the SLR impact model ($\tan(\alpha)$ and $\tan(\beta)$). The Bruun model slope ($\tan(\alpha)$) is determined by the limits of the active beach profile. Local scale bathymetric surveys are scarce on most sandy coasts and do not allow for a reliable validation of the seaward limit of the active beach profile. The available global wave and topo-bathymetric merged datasets and local scale bathymetric surveys currently allow for estimates of $\tan(\alpha)$ [59]. However, the accuracy of such data is limited owing to the spatiotemporal variability of the available merged data, merging procedures and estimation of the depth of closure [59,60]. Therefore, the Bruun slope $\tan(\alpha)$ is typically associated to large uncertainties [24,28,61]. The foreshore beach slope, which is adopted in the current model, does not require the estimation of active beach boundaries and can be extracted from topographic profiles (regular enough to account for potential temporal and spatial variability) that can be more easily surveyed by various means at a low cost. Further, recently developed satellite-remote sensing techniques to derive foreshore beach slopes over large scales [62] may represent a promising complement to the model developed here. Thus, the ESMs combined with SLR-driven recession (including feedbacks) may result in reduced uncertainty in long-term shoreline change and a potential of application to a much wider range of coasts compared to the models based on the linear sum of the Bruun and ESM projections.

5.4. Beyond the Bruun Rule

The conceptualization of SLR-driven erosion provided in this contribution identifies the wave-reshaping process as a key component of this mechanism. The derivation of the

wave-efficiency change requires an assumption on the complex interaction between the waves and the changing sea level, which amplifies the impact of the waves on the shoreline position. In this paper, the SLR-induced disequilibrium that drives wave-reshaping erosion is quantified based on the assumption that such disequilibrium corresponds to the effect of passive flooding on the shoreline. Future research efforts may aim at providing a generalized physics-based expression of this disequilibrium, for instance by investigating wave energy dissipation change in response to the changing bottom slope. For instance, Davidson [63] recently proposed a model where the influence of the changing sea level and bottom slope on wave energy dissipation is accounted.

It is to be noted that the aim of this paper is to present a proof of concept, and the next challenges include a validation of the concept against observations. Such validation would require a long-term (e.g., decadal) time series of accurate shoreline position (for calibration purposes) with persistent low-energy incident waves (e.g., <1m), a fast-changing relative sea level (of the order of centimeters per year) and a relatively stable sediment budget to depict SLR impacts at a given field site. To the best of the authors' knowledge, such dataset does not exist. Another avenue is to address the impact of sea-level anomalies of the order of tenths of centimeters on time scales of weeks to months, as observed off the coast of Japan [64] or in El Niño Southern Oscillation [65], associated with frequent shoreline measurements. Alternatively, laboratory data produced during reduced scale studies assessing the effects of SLR [6,7] may be used for the validation of the present framework.

6. Conclusions

The Bruun Rule is increasingly used in current coastal impact models, whether standalone (regional to global scale) or coupled to ESMs (local scale), often without full consideration of its underlying physics. This paper introduces a new interpretation of the SLR-driven shoreline response mechanism based on equilibrium beach theory, identifying two main contributing processes: passive flooding and wave reshaping. It is shown that, when Bruun's assumptions are satisfied, the proposed conceptualization provides a physics-based background to the Bruun model. Our concept also provides support to the integration of SLR impact into ESMs for future studies, and new ground for the development of more generalized shoreline models. We also showed that ESMs can be used to explicitly compute the portion of sea-level-driven shoreline change induced by the change in wave-erosion efficiency. In particular, using a disequilibrium condition based on the current shoreline position can be efficiently coupled (with feedback) with the SLR-induced passive flooding. Such modeling does not require the knowledge of the active profile (Bruun) slope but, instead, the foreshore slope, which can be easily measured and is typically associated with less uncertainties than the Bruun slope. This can ultimately avoid bias in long-term shoreline projection considering climate change and the sea-level rise.

We addressed the coupling of SLR-driven erosion with ESMs, for cross-shore-transport-dominated coasts. However, our analysis also holds for the new generation of hybrid models that couple ESM with other transport processes (e.g., longshore transport), local geology and/or the backing coastal dunes (e.g., [17,36,38,66]), and to ESMs that continuously adapt the shoreline response to the non-stationary wave climate through time-varying model parameters [52]. In such models, not only SLR but also other processes can affect shoreline position and, in turn, the equilibrium profile conditions. We therefore anticipate that our findings will help future studies addressing the long-term evolution of wave-dominated sandy coasts as sea level rises.

Supplementary Materials: The following are available online at https://www.mdpi.com/article/10.3390/jmse9090974/s1, Table S1: List of symbols and notations used in this paper, Table S2: List of acronyms used in this paper.

Author Contributions: M.D.: Conceptualization, methodology, formal analysis, writing—original draft; D.I.: funding acquisition, supervision, writing—review & editing; B.C.: investigation, supervision, resources, writing—review & editing; S.V.: investigation, writing—review & editing; G.L.C.:

investigation, writing— review & editing. All authors have read and agreed to the published version of the manuscript.

Funding: This work is supported by the MOGPA (Make Our Planet Great Again), grant no. [927923G], as well as BRGM. BC is funded by the Agence Nationale de la Recherche (ANR) through grant [ANR-147-CE01-0014] (SONO project). GLC is supported by the ERA4CS INSeaPTION Grant [690462].

Institutional Review Board Statement: Not applicable.

Informed Consent Statement: Not applicable.

Data Availability Statement: This study includes the beach monitoring data study of Truc Vert labeled by the Service National d'Observation (SNO) Dynalit (https://www.dynalit.fr), with additional support from Observatoire Aquitaine de l'Univers (OASU) and Observatoire de la Côte Aquitaine (OCA).

Acknowledgments: The authors thank their colleagues, including S. Bujan, S. Ferreira and V. Marieu, involved in the topographic data, and J. Rohmer and R. Thiéblemont for earlier discussions.

Conflicts of Interest: The authors declare no conflict of interest.

Appendix A. Passive Flooding, Wave Reshaping and the Bruun Rule

In this Appendix we show how expressing the Bruun Rule as the long-term cumulated effects of passive flooding and wave reshaping implies constant mean rates of these two contributions over time. The physical mechanism proposed in Section 2.2 indicates that SLR induces a shoreline change driven by the cumulated effects of passive flooding (S_{PF}) and wave reshaping (S_{WR}) over a time T:

$$S_{PF} + S_{WR} = \int_T dS_{PF}dt + \int_T dS_{WR}dt \tag{A1}$$

When the Bruun Rule assumptions (Section 2.1) are satisfied, namely the assumption of stationary long-term wave climate and constant SLR rate, over periods associating no trends in wave climate (e.g., $dT \geq$ O(year)), the mean rates of passive flooding and wave reshaping effects are constant over time:

$$\overline{dS_{PF}} + \overline{dS_{WR}} = \frac{1}{dT}\int_{dT} dS_{PF}dt + \frac{1}{dT}\int_{dT} dS_{WR}dt = c_1 + c_2 \tag{A2}$$

Hence, over a time $\Delta T = n\,dT$ (with n positive integer), Equation (A1) becomes:

$$S_{PF} + S_{WR} = \int_{\Delta T} dS_{PF}dt + \int_{\Delta T} dS_{WR}dt = \overline{dS_{PF}}\Delta T + \overline{dS_{WR}}\Delta T \tag{A3}$$

Therefore, under these specific conditions, on the time scale of dT (years or longer), the Bruun Rule can be expressed in terms of cumulated passive flooding and wave reshaping effects, as follows:

$$S_{Bruun} = \frac{SLR}{\tan(\alpha)} = S_{PF} + S_{WR} = \overline{dS_{PF}}\Delta T + \overline{dS_{WR}}\Delta T \tag{A4}$$

Appendix B. Integrating SLR-Driven Disequilibrium into ESMs with Feedback

In this Appendix, we provide a more detailed description of the approach introduced in Section 3.2, where SLR-driven erosion and an ESM based on the current shoreline position are integrated, enabling feedback between SLR effects and the disequilibrium condition. Then, we further analyze the assumption used to quantify the disequilibrium induced by sea-level rise (SLR), and we analytically show that such assumption is consistent with the Bruun model structure.

Given an ESM based on the current shoreline position, if the equilibrium energy in Equation (5) ($E_{eq} = E_{eq}\,(S)$) is expressed by a linear relationship between incident wave energy (E) and current shoreline cross-shore distance from a given reference (S) (i.e., $E_{eq} =$

$aS + b$, after Yates et al. [9]), the instantaneous disequilibrium state can be represented on the S-E Cartesian plane (Figure A1). In Figure A1a, a given shoreline position is associated with an equilibrium wave energy (E_{eq}) that would not produce a shoreline change (black solid line), while positions located above and below the equilibrium line are associated with erosion ($dS/dt < 0$, red points) and accretion ($dS/dt > 0$, blue points), respectively. An increase in MSL (dMSL) induces passive flooding (dS_{PF}), corresponding to a landward shift of the reference shoreline (Figure 3b of the main text), i.e., a smaller S value. Recall that this shift represents only a translation of the reference system with no morphologic changes to the beach profile. Therefore, the effect of passive flooding is projected on the S-E plane as a landward shift of the equilibrium shoreline position (red arrows and red point in Figure A1b). The second consequence of dMSL (observed in Figure 3b of the main text) is a general increase in the bottom slope relative to the local wave climate propagating over the new MSL. In morphologic terms, in respect to a given equilibrium profile, a generally steeper beach profile is closer to equilibrium with low energy wave conditions and farther to high energy wave conditions [31], resulting in an overall (erosive) disequilibrium of the beach–wave climate system (Figure 3c of the main text). As the equilibrium condition is defined in terms of wave energy (E), the SLR-induced disequilibrium is projected on the S-E plane as a downward shift of the equilibrium line ($dE_{eq,SLR}$ and dashed black line in Figure A1b), indicating that for a given shoreline position (S) less wave energy is required to erode the beach and restore the equilibrium. Or, alternatively, for a given wave climate, the efficiency of erosion is increased, which can result from an increased depth and bottom slope across the beach profile due to SLR and wave breaking tending to occur closer to the shore.

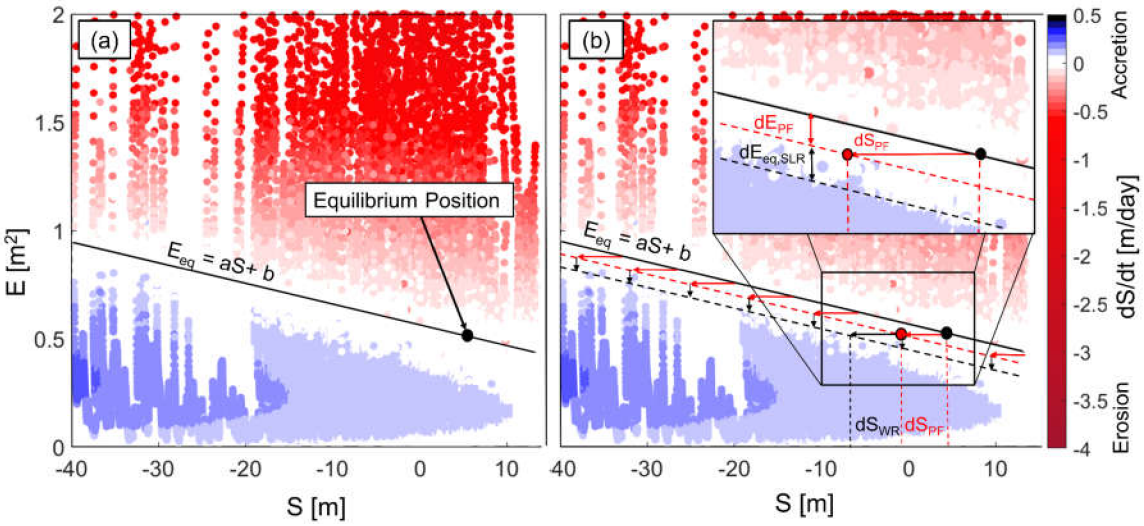

Figure A1. Example of shoreline position (S) vs. incident wave energy density (E = 1/16 H_s^2, where H_s is the significant wave height) Cartesian plane, with the linear equilibrium beach-wave condition following Yates et al. [9] (solid black line). The color-bar indicates the magnitude of potential erosion (red) and accretion (blue). Red arrows indicate the geometric shift due to Passive Flooding (dS_{PF}); vertical black arrows indicate the disequilibrium change ($dE_{eq,SLR}$) corresponding to the change in the bottom slope relative to MSL; and the horizontal black arrow indicates the potential Wave Reshaping effect (dS_{WR}) that would re-establish the equilibrium state. The black dash line indicates the new equilibrium beach–wave condition post-SLR. The data used for this example refer to Truc Vert beach (France).

Quantifying $dE_{eq,SLR}$ is not straightforward. To our knowledge, the literature does not provide a physical expression of the increase in wave-driven erosion efficiency as a function of SLR. Therefore, to go one step further in the quantification of this complex interaction, we make the reasonable (though approximate) assumption that the increase in wave efficiency ($dE_{eq,SLR}$) has the same magnitude as the apparent wave-energy increase associated with the passive flooding shift on the S-E plane ($dE_{PF} = -a\, dS_{PF}$ in Figure A1b). Hence, for a given wave energy, additional erosion must occur and, consequently, the

magnitude of this wave-efficiency-driven erosion (dS_{WR}) is the same as dS_{PF}. The latter implication is consistent with the Bruun Rule's structure, as demonstrated below.

Given that $E_{eq} = aS + b$, the increase in disequilibrium ($dE_{eq,SLR}$) that results in dS_{WR} is:

$$dE_{eq,SLR} = -a\, dS_{WR} \tag{A5}$$

The Bruun Rule can be expressed in terms of passive flooding and wave reshaping, as follows:

$$S_{Bruun} = \frac{SLR}{\tan(\alpha)} = S_{PF} + S_{WR} \tag{A6}$$

As described in Section 2.2, the passive flooding contribution can be computed as:

$$S_{PF} = \frac{SLR}{\tan(\beta)} \tag{A7}$$

Where tan (β) is the slope of the beach foreshore.

In order for the combined recession to be consistent with the Bruun Rule recession (Equation (A6)), S_{WR} can be expressed as:

$$S_{WR} = cS_{PF} = c\frac{SLR}{\tan(\beta)} \tag{A8}$$

And substituted into Equation A6 to give

$$\frac{SLR}{\tan(\alpha)} = \frac{SLR}{\tan(\beta)} + c\frac{SLR}{\tan(\beta)} \tag{A9}$$

$$\frac{SLR}{\tan(\alpha)} = \frac{SLR}{\tan(\beta)}(1 + c) \tag{A10}$$

$$c = \frac{\tan(\beta)}{\tan(\alpha)} - 1 \tag{A11}$$

Thus, expressing Equation (A8) in incremental terms (dS_{WR} and dS_{PF}), substituting the result into Equation (A5), we obtain

$$dE_{eq,SLR} = -a\, dS_{WR} = -a\, c\, dS_{PF} \tag{A12}$$

and, assuming $c = 1$ ($(\tan(\beta))/(\tan(\alpha)) = 2$), we obtain

$$dE_{eq,SLR} = -a\, dS_{PF} = dE_{PF} \tag{A13}$$

Recall that, while realistic, the assumption described herein (Equation (A13)) is only used to provide an approximate quantification of $dE_{eq,SLR}$. Here, we adopt Equation (A13) in order to analyze the behavior of an ESM where feedbacks between the modeled processes are enabled, but it may not be applicable in the generality of cases in practice.

In Section 3.2 of the main text, we proposed an approach for integrating SLR-driven recession into ESMs based on the current shoreline position, where feedbacks between modeled processes are allowed. In particular, we focused on ESMs where the equilibrium condition is expressed as $E_{eq} = aS + b$.

For this case, if SLR is applied at a given time step, the consequent dS_{PF} is added on the short-term to the ESM, accounting for the shoreline reference retreat induced by passive flooding. This first (geometric) effect of passive flooding is accounted in the equilibrium condition as a landward shift of the reference shoreline position (Figure A1). The second effect of SLR (and thus passive flooding) is a disequilibrium increase due to the apparent

increase in the beach profile slope, which ultimately results in dS_{WR}. Therefore, the new equilibrium condition (E^*_{eq}) can be rewritten as:

$$E^*_{eq} = a\left(S - \sum dS_{PF}\right) + b + \sum dE_{eq,SLR} \quad \text{(A14)}$$

where the term "ΣdS_P" represents the cumulative landward shift of the reference shoreline position, while the term "$\Sigma dE_{eq,SLR}$" quantifies the cumulative disequilibrium change induced by SLR.

Under the assumption described above, the disequilibrium increase ($dE_{eq,SLR}$) can be expressed by Equation (A5) and can be injected in Equation (A14), giving:

$$E^*_{eq} = a\left(S - 2\sum dS_{PF}\right) + b \quad \text{(A15)}$$

Recall that although the additional SLR-induced disequilibrium is expressed as a function of dS_{PF}, the dS_{WR} resulting from it is of a different nature (Section 2.2). In response to the altered disequilibrium, the model captures the contribution of waves at each modeled time step to profile reshaping (dS_{WR}). In this approach, the effect of SLR is included correctly by adding the sole dS_{PF} term to the ESM and using the equilibrium condition in Equation (A13):

$$dS = k^{+/-}F\left\{\left[a\left(S - 2\sum dS_{PF}\right) + b\right] - E\right\}dt + dS_{PF} \quad \text{(A16)}$$

The presence of the dS_{PF} term in Equation (A16) is so that the shoreline adjusts instantly to the passive flooding and evolves over time due to wave reshaping, consistently with the conceptual model.

We note that the magnitude of dS_{WR} at each time step is quantified in Equation (A16) as a function of the sea-level-driven disequilibrium change and the instantaneous wave intensity, as follows:

$$dS_{WR} = k^{+/-}F\, dE_{eq,SLR}\, dt \quad \text{(A17)}$$

References

1. Ranasinghe, R. Assessing climate change impacts on open sandy coasts: A review. *Earth-Sci. Rev.* **2016**, *160*, 320–332. [CrossRef]
2. Oppenheimer, M.; Glavovic, B.; Hinkel, J.; van de Wal, R.; Magnan, A.K.; Abd-Elgawad, A.; Cai, R.; Cifuentes-Jara, M.; Deconto, R.M.; Ghosh, T.; et al. Sea level rise and implications for low-lying islands, coasts and communities. In *IPCC Special Report on the Ocean and Cryosphere in a Changing Climate*; Pörtner, H.-O., Roberts, D., Masson-Delmotte, V., Zhai, P., Tignor, M., Poloczanska, E., Mintenbeck, K., Alegría, A., Nicolai, M., Okem, A., Eds.; 2019.
3. Toimil, A.; Camus, P.; Losada, I.J.; Le Cozannet, G.; Nicholls, R.J.; Idier, D.; Maspataud, A. Climate change-driven coastal erosion modelling in temperate sandy beaches: Methods and uncertainty treatment. *Earth-Sci. Rev.* **2020**, *202*, 103110. [CrossRef]
4. Vitousek, S.; Barnard, P.L.; Limber, P. Can beaches survive climate change? *J. Geophys. Res. Earth Surf.* **2017**, *122*, 1060–1067. [CrossRef]
5. Bruun, P. Sea-level rise as a cause of shore erosion. *J. Waterw. Harb. Div.* **1962**, *88*, 117–130. [CrossRef]
6. Atkinson, A.L.; Baldock, T.E.; Birrien, F.; Callaghan, D.P.; Nielsen, P.; Beuzen, T.; Turner, I.L.; Blenkinsopp, C.E.; Ranasinghe, R. Laboratory investigation of the Bruun Rule and beach response to sea level rise. *Coast. Eng.* **2018**, *136*, 183–202. [CrossRef]
7. Bayle, P.M.; Beuzen, T.; Blenkinsopp, C.E.; Baldock, T.E.; Turner, I.L. Beach profile changes under sea level rise in laboratory flume experiments at different scale. *J. Coast. Res.* **2020**, *95*, 192–196. [CrossRef]
8. Miller, J.K.; Dean, R.G. A simple new shoreline change model. *Coast. Eng.* **2004**, *51*, 531–556. [CrossRef]
9. Yates, M.L.; Guza, R.T.; O'Reilly, W.C. Equilibrium shoreline response: Observations and modeling. *J. Geophys. Res.* **2009**, *114*. [CrossRef]
10. Davidson, M.A.; Splinter, K.D.; Turner, I.L. A simple equilibrium model for predicting shoreline change. *Coast. Eng.* **2013**, *73*, 191–202. [CrossRef]
11. Splinter, K.D.; Turner, I.L.; Davidson, M.A.; Barnard, P.; Castelle, B.; Oltman-Shay, J. A generalized equilibrium model for predicting daily to interannual shoreline response. *J. Geophys. Res. Earth Surf.* **2014**, *119*, 1936–1958. [CrossRef]
12. Jara, M.S.; González, M.; Medina, R. Shoreline evolution model from a dynamic equilibrium beach profile. *Coast. Eng.* **2015**, *99*, 1–14. [CrossRef]
13. Castelle, B.; Marieu, V.; Bujan, S.; Ferreira, S.; Parisot, J.-P.; Capo, S.; Sénéchal, N.; Chouzenoux, T. Equilibrium shoreline modelling of a high-energy meso-macrotidal multiple-barred beach. *Mar. Geol.* **2014**, *347*, 85–94. [CrossRef]

14. Lemos, C.; Floc'h, F.; Yates, M.; Le Dantec, N.; Marieu, V.; Hamon, K.; Cuq, V.; Suanez, S.; Delacourt, C. Equilibrium modeling of the beach profile on a macrotidal embayed low tide terrace beach. *Ocean. Dyn.* **2018**, *68*, 1207–1220. [CrossRef]
15. Banno, M.; Kuriyama, Y.; Hashimoto, N. Equilibrium-based foreshore beach profile change model for long-term data. In *The Proceedings of the Coastal Sediments 2015*; World Scientific: Singapore, 2015. [CrossRef]
16. Dean, R.G.; Houston, J.R. Determining shoreline response to sea level rise. *Coast. Eng.* **2016**, *114*, 1–8. [CrossRef]
17. Vitousek, S.; Barnard, P.L.; Limber, P.; Erikson, L.; Cole, B. A model integrating longshore and cross-shore processes for predicting long-term shoreline response to climate change. *J. Geophys. Res. Earth Surf.* **2017**, *122*, 782–806. [CrossRef]
18. D'Anna, M.; Idier, D.; Castelle, B.; Le Cozannet, G.; Rohmer, J.; Robinet, A. Impact of model free parameters and sea-level rise uncertainties on 20-years shoreline hindcast: The case of Truc Vert beach (SW France). *Earth Surf. Process. Landf.* **2020**, *45*, 1895–1907. [CrossRef]
19. D'Anna, M.; Castelle, B.; Idier, D.; Rohmer, J.; Le Cozannet, G.; Thieblemont, R.; Bricheno, L. Uncertainties in shoreline projections to 2100 at Truc Vert beach (France): Role of sea-level rise and equilibrium model assumptions. *J. Geophys. Res. Earth Surf.* **2021**, *126*, e2021JF006160. [CrossRef]
20. Bruun, P. Review of conditions for uses of the Bruun Rule of erosion. *Coast. Eng.* **1983**, *7*, 77–89. [CrossRef]
21. Bruun, P. The Bruun Rule of erosion by sea-level rise: A discussion on large-scale two- and three-dimensional usages. *J. Coast. Res.* **1988**, *4*, 627–648.
22. Dean, R.G. Equilibrium beach profiles: Characteristics and applications. *J. Coast. Res.* **1991**, *7*, 53–84.
23. Hallermeier, R.J. Uses for a calculated limit depth to beach erosion. In Proceedings of the 16th Coastal Engineering Conference; ASCE: New York, NY, USA, 1978; pp. 1493–1512.
24. Nicholls, R.J. Assessing erosion of sandy beaches due to sea-level rise. *Geol. Soc. Lond. Eng. Geol. Spec. Publ.* **1998**, *15*, 71–76. [CrossRef]
25. Anderson, T.R.; Fletcher, C.H.; Barbee, M.M.; Romine, B.M.; Lemmo, S.; Delevaux, J.M.S. Modeling multiple sea level rise stresses reveals up to twice the land at risk compared to strictly passive flooding methods. *Sci. Rep.* **2018**, *8*, 1–14. [CrossRef] [PubMed]
26. Davidson-Arnott, R.G.D. Conceptual model of the effects of sea level rise on sandy coasts. *J. Coast. Res.* **2005**, *216*, 1166–1172. [CrossRef]
27. Cooper, J.A.G.; Pilkey, O.H. Sea-level rise and shoreline retreat: Time to abandon the Bruun Rule. *Glob. Planet. Chang.* **2004**, *43*, 157–171. [CrossRef]
28. Ranasinghe, R.; Callaghan, D.; Stive, M.J.F. Estimating coastal recession due to sea level rise: Beyond the Bruun rule. *Clim. Chang.* **2012**, *110*, 561–574. [CrossRef]
29. Rosati, J.D.; Dean, R.G.; Walton, T.L. The modified Bruun Rule extended for landward transport. *Mar. Geol.* **2013**, *340*, 71–81. [CrossRef]
30. Wolinsky, M.A.; Murray, A.B. A unifying framework for shoreline migration: 2. Application to wave-dominated coasts. *J. Geophys. Res. Earth Surf.* **2009**, *114*. [CrossRef]
31. Wright, L.; Short, A. Morphodynamic variability of surf zones and beaches: A synthesis. *Mar. Geol.* **1984**, *56*, 93–118. [CrossRef]
32. Falqués, A.; Garnier, R.; Ojeda, E.; Ribas, F.; Guillen, J. Q2D-morfo: A medium to long term model for beach morphodynamics. *Coast. Estuar. Morphoynamics* **2007**, *1*, 71–78.
33. Toimil, A.; Losada, I.J.; Camus, P.; Díaz-Simal, P. Managing coastal erosion under climate change at the regional scale. *Coast. Eng.* **2017**, *128*, 106–122. [CrossRef]
34. Robinet, A.; Idier, D.; Castelle, B.; Marieu, V. A reduced-complexity shoreline change model combining longshore and cross-shore processes: The LX-Shore model. *Environ. Model. Softw.* **2018**, *109*, 1–16. [CrossRef]
35. Vitousek, S.; Cagigal, L.; Montaño, J.; Rueda, A.; Mendez, F.; Coco, G.; Barnard, P.L. The application of ensemble wave forcing to quantify uncertainty of shoreline change predictions. *J. Geophys. Res. Earth Surf.* **2021**, *126*. [CrossRef]
36. Robinet, A.; Castelle, B.; Idier, D.; D'Anna, M.; Le Cozannet, G. Simulating the impact of sea-level rise and offshore bathymetry on embayment shoreline changes. *J. Coast. Res.* **2020**, *95*, 1263–1267. [CrossRef]
37. Jaramillo, C.; Jara, M.S.; González, M.; Medina, R. A shoreline evolution model considering the temporal variability of the beach profile sediment volume (sediment gain/loss). *Coast. Eng.* **2020**, *156*, 103612. [CrossRef]
38. Antolínez, J.A.A.; Méndez, F.J.; Anderson, D.; Ruggiero, P.; Kaminsky, G.M. Predicting climate-driven coastlines with a simple and efficient multiscale model. *J. Geophys. Res. Earth Surf.* **2019**, *124*, 1596–1624. [CrossRef]
39. Robinet, A.; Castelle, B.; Idier, D.; Le Cozannet, G.; Déqué, M.; Charles, E. Statistical modeling of interannual shoreline change driven by North Atlantic climate variability spanning 2000–2014 in the Bay of Biscay. *Geo-Mar. Lett.* **2016**, *36*, 479–490. [CrossRef]
40. Larson, M.; Hoan, L.X.; Hanson, H. Direct formula to compute wave height and angle at incipient breaking. *J. Waterw. Port Coast. Ocean. Eng.* **2010**, *136*, 119–122. [CrossRef]
41. Thiéblemont, R.; Le Cozannet, G.; Toimil, A.; Meyssignac, B.; Losada, I.J. Likely and high-end impacts of regional sea-level rise on the shoreline change of European sandy coasts under a high greenhouse gas emissions scenario. *Water* **2019**, *11*, 2607. [CrossRef]
42. Yates, M.L.; Guza, R.T.; O'Reilly, W.C.; Hansen, J.E.; Barnard, P.L. Equilibrium shoreline response of a high wave energy beach. *J. Geophys. Res. Ocean.* **2011**, *116*. [CrossRef]
43. Ludka, B.C.; Guza, R.T.; O'Reilly, W.C.; Yates, M.L. Field evidence of beach profile evolution toward equilibrium. *J. Geophys. Res. Ocean.* **2015**, *120*, 7574–7597. [CrossRef]
44. Bertsimas, D.; Tsitsiklis, J. Simulated annealing. *Stat. Sci.* **1993**, *8*, 20–69. [CrossRef]

45. Castelle, B.; Bujan, S.; Marieu, V.; Ferreira, S. 16 years of topographic surveys of rip-channelled high-energy meso-macrotidal sandy beach. *Sci. Data* **2020**, *7*, 410. [CrossRef] [PubMed]
46. Banno, M.; Kuriyama, Y. Supermoon drives beach morphological changes in the swash zone. *Geophys. Res. Lett.* **2020**, *47*, e2020GL089745. [CrossRef]
47. SCOR Working group 89. The response of beaches to sea-level changes: A review of predictive models. *J. Coast. Res.* **1991**, *7*, 895–921.
48. Stive, M.; Ranasinghe, R.; Cowell, P.J. Sea level rise and coastal erosion. In *Handbook of Coastal and Ocean Engineering*; Kim, Y., Ed.; World Scientific: Singapore, 2010; pp. 1023–1037.
49. Cooper, J.A.G.; Masselink, G.; Coco, G.; Short, A.D.; Castelle, B.; Rogers, K.; Anthony, E.; Green, A.N.; Kelley, J.T.; Pilkey, O.H.; et al. Sandy beaches can survive sea-level rise. *Nat. Clim. Chang.* **2020**, *10*, 993–995. [CrossRef]
50. Morim, J.; Hemer, M.; Wang, X.L.; Cartwright, N.; Trenham, C.; Semedo, A.; Young, I.; Bricheno, L.; Camus, P.; Casas-Prat, M.; et al. Robustness and uncertainties in global multivariate wind-wave climate projections. *Nat. Clim. Chang.* **2019**, *9*, 711–718. [CrossRef]
51. Splinter, K.D.; Turner, I.L.; Reinhardt, M.; Ruessink, G. Rapid adjustment of shoreline behavior to changing seasonality of storms: Observations and modelling at an open-coast beach. *Earth Surf. Process. Landf.* **2017**, *42*, 1186–1194. [CrossRef]
52. Ibaceta, R.; Splinter, K.D.; Harley, M.D.; Turner, I.L. Enhanced coastal shoreline modeling using an ensemble kalman filter to include nonstationarity in future wave climates. *Geophys. Res. Lett.* **2020**, *47*, e2020GL090724. [CrossRef]
53. Splinter, K.D.; Turner, I.L.; Davidson, M.A. How much data is enough? The importance of morphological sampling interval and duration for calibration of empirical shoreline models. *Coast. Eng.* **2013**, *77*, 14–27. [CrossRef]
54. Ruessink, B.G. Predictive uncertainty of a nearshore bed evolution model. *Cont. Shelf Res.* **2005**, *25*, 1053–1069. [CrossRef]
55. Simmons, J.A.; Harley, M.D.; Marshall, L.A.; Turner, I.L.; Splinter, K.D.; Cox, R.J. Calibrating and assessing uncertainty in coastal numerical models. *Coast. Eng.* **2017**, *125*, 28–41. [CrossRef]
56. Kroon, A.; de Schipper, M.A.; van Gelder, P.H.A.J.M.; Aarninkhof, S.G.J. Ranking uncertainty: Wave climate variability versus model uncertainty in probabilistic assessment of coastline change. *Coast. Eng.* **2020**, *158*, 103673. [CrossRef]
57. Cagigal, L.; Rueda, A.; Anderson, D.; Ruggiero, P.; Merrifield, M.A.; Montaño, J.; Coco, G.; Méndez, F.J. A multivariate, stochastic, climate-based wave emulator for shoreline change modelling. *Ocean. Model.* **2020**, *154*, 101695. [CrossRef]
58. Pringle, J.; Stretch, D.D. On a new statistical wave generator based on atmospheric circulation patterns and its applications to coastal shoreline evolution. *Comput. Geosci.* **2021**, *149*, 104707. [CrossRef]
59. Athanasiou, P.; van Dongeren, A.; Giardino, A.; Vousdoukas, M.; Gaytan-Aguilar, S.; Ranasinghe, R. Global distribution of nearshore slopes with implications for coastal retreat. *Earth Syst. Sci. Data* **2019**, *11*, 1515–1529. [CrossRef]
60. Athanasiou, P.; van Dongeren, A.; Giardino, A.; Vousdoukas, M.I.; Ranasinghe, R.; Kwadijk, J. Uncertainties in projections of sandy beach erosion due to sea level rise: An analysis at the European scale. *Sci. Rep.* **2020**, *10*, 1–14. [CrossRef] [PubMed]
61. Le Cozannet, G.; Oliveros, C.; Castelle, B.; Garcin, M.; Idier, D.; Pedreros, R.; Rohmer, J. Uncertainties in sandy shorelines evolution under the Bruun Rule assumption. *Front. Mar. Sci.* **2016**, *3*, 49. [CrossRef]
62. Vos, K.; Harley, M.D.; Splinter, K.D.; Walker, A.; Turner, I.L. Beach slopes from satellite-derived shorelines. *Geophys. Res. Lett.* **2020**, *47*, e2020GL088365. [CrossRef]
63. Davidson, M. Forecasting coastal evolution on time-scales of days to decades. *Coast. Eng.* **2021**, *168*, 103928. [CrossRef]
64. Banno, M.; Nakamura, S.; Kosako, T.; Nakagawa, Y.; Yanagishima, S.; Kuriyama, Y. Long-Term observations of beach variability at Hasaki, Japan. *J. Mar. Sci. Eng.* **2020**, *8*, 871. [CrossRef]
65. Barnard, P.L.; Hoover, D.; Hubbard, D.M.; Snyder, A.; Ludka, B.C.; Allan, J.; Kaminsky, G.M.; Ruggiero, P.; Gallien, T.W.; Gabel, L.; et al. Extreme oceanographic forcing and coastal response due to the 2015–2016 El Niño. *Nat. Commun.* **2017**, *8*, 14365. [CrossRef] [PubMed]
66. Tran, Y.H.; Barthélemy, E. Combined longshore and cross-shore shoreline model for closed embayed beaches. *Coast. Eng.* **2020**, *158*, 103692. [CrossRef]